

Long range crossed Andreev reflections in high T_c superconductors

William J. Herrera

Departamento de Física, Universidad Nacional de Colombia, Bogotá, Colombia.

A. Levy Yeyati and A. Martín-Rodero

*Departamento de Física Teórica de la Materia Condensada,
Universidad Autónoma de Madrid,
E-28049 Madrid, Spain.*

(Dated: May 27, 2018)

We analyze the non-local transport properties of a d -wave superconductor coupled to metallic electrodes at nanoscale distances. We show that the non-local conductance exhibits an algebraical decay with distance rather than the exponential behavior which is found in conventional superconductors. Crossed Andreev processes, associated with electronic entanglement, are favored for certain orientations of the symmetry axes of the superconductor with respect to the leads. These properties would allow its experimental detection using present technologies.

PACS numbers: 74.20.Rp, 74.50.+r, 74.45.+c, 81.07.Lk

I. INTRODUCTION

Cooper pairs in superconducting nanostructures provide a potential source of entangled electrons [1, 2, 3, 4, 5], a possibility that has been recently explored in conventional superconductors both theoretically [6, 7, 8, 9, 10, 11, 12, 13, 14, 15, 16] and experimentally [17, 18, 19, 20]. In a typical experimental device, a superconducting region is contacted by several metallic electrodes at nanoscale distances with the aim of analyzing the non-local transport properties at subgap voltages. In the limit of vanishing contact transparency the non-local conductance is controlled by two type of processes yielding opposite contributions: direct elastic tunneling of electrons between two separate leads (elastic cotunneling, EC) and crossed Andreev reflection (CAR) processes in which injected electrons from one lead are reflected as holes in the other lead (see Fig. 1). The time reverse of these last processes involve entangled electron pairs on two separate leads [21]. In conventional superconductors the average conductance tends to cancel due to the opposite contribution of EC and CAR processes [8, 9]. Several mechanisms have been proposed to avoid a complete cancellation and have been invoked to explain the available experimental results. Among them one can quote the use of ferromagnetic leads [7, 10, 11, 12] and the effect of electron-electron interactions in certain experimental geometries [15]. On the other hand, the magnitude of these non-local processes decays exponentially with the distance between the leads on a scale fixed by the superconducting coherence length ξ_0 . In practice this means that non-local effects can be observed on distances of the order 10 nm to $1\mu\text{m}$, depending on the material [17, 18].

These effects have been much less explored in the case of unconventional high critical temperature superconductors (HTcS)[6, 22, 23]. The characteristic small values of the coherence length in these systems cast doubts about the observability of non-local correlations. However, due

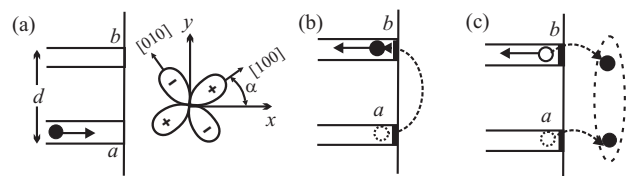


FIG. 1: Two leads on a d -wave superconductor. The distance between the leads is d , α is the angle between the crystallographic axes of the superconductor and the direction normal to the surface. An incoming electron from lead a can be reflected in lead b as: (b) an electron or, (c) a hole while a Cooper pair is created in the superconductor.

to the anisotropy of the pair potential, the coherence length along certain directions can be much larger than ξ_0 . This anisotropy is behind the non-local nature of the electromagnetic response of HTcS[24, 25]. In fact, some indirect evidence of CAR processes in HTcS coupled to ferromagnetic leads has been presented [26, 27].

In the present work we analyze the non-local transport in d -wave superconductors and show that in contrast to the conventional s -wave case, CAR processes are long ranged. Moreover, we show that for certain orientations of the axes of the superconductor with respect to the contacts, CAR processes dominate over EC at low voltages and small contact transparency. We believe that these findings open the possibility of using HTcS as a source of entangled electron pairs.

II. CROSSED ANDREEV REFLECTION AND ELASTIC COTUNNELING IN HIGH T_C SUPERCONDUCTORS

The situation to be analyzed is illustrated in Fig. 1. We consider a semi-infinite d -wave superconducting re-

gion connected to two normal leads, denoted by a and b , and separated a distance d . Our aim is finding the current induced on lead b , I_b , when a voltage V_a is applied on lead a . The two processes contributing to this current are depicted on panels (b) and (c). Being the result of the diffraction of quasiparticles by an anisotropic pair potential, the relative weight of the two processes will be affected by the orientation of the superconductor symmetry axis (angle α in Fig. 1). In fact, EC processes are favored for electron propagation along the nodal lines (where the order parameter vanishes), while CAR processes reach a maximum amplitude along directions where the modulus of the pair potential is maximum. Although on a spatial average the contribution of the two processes should be equal as in the case of isotropic s-wave superconductors, a dominance of one of the two can be found for specific orientations of the symmetry axis with respect to the leads. These qualitative arguments allow to understand the dominance of CAR over EC processes for the $\alpha = 0$ case ($d_{x^2-y^2}$ symmetry) and the opposite behavior in the case of $\alpha = \pi/4$ (d_{xy} symmetry) as discussed in detail below.

In the spirit of the Hamiltonian approach of Ref. [28] the differential conductance defined as $\sigma_{ba} = dI_b/dV_a$, can be written as [10]

$$\sigma_{ba} = \frac{8\pi^2 e p_a^2 p_b^2}{h} \rho_{e,a}(\rho_{h,b} |G_{ba,12}^r(eV)|^2 - \rho_{e,b} |G_{ba,11}^r(eV)|^2), \quad (1)$$

where $\rho_{e(h),a(b)}$ is the local density of states of the electron(hole) in the lead $a(b)$, while p_a and p_b denote the corresponding hopping parameters coupling the superconductor to the leads. The quantities $G_{ba,11}^r(eV)$ and $G_{ba,12}^r(eV)$ are the non-local propagators in the superconducting region (indexes 1,2 refer to electrons and holes in Nambu space). The first term on the right hand side of Eq. (1) is due to CAR processes, while the second term corresponds to EC. Therefore the crossed differential conductance is positive if CAR dominates over EC or negative in the opposite case. In order to make contact with possible experiments it also convenient to analyze the non-local resistance R_{ba} , given by $-\sigma_{ba}/(\sigma_{aa}\sigma_{bb} - \sigma_{ab}\sigma_{ba})$, where $\sigma_{aa(bb)}$ are the local conductances which can be obtained within the same formalism [10, 28]. The propagators $G_{\alpha\beta,ij}^r$ of the coupled system are then given by $\check{G}^r(E) = (\check{g}^r(E)^{-1} + i\check{\Gamma})^{-1}$, where \check{g}^r is the retarded Green function of the uncoupled superconductor and $\check{\Gamma}_{\alpha\beta,ij} = p_\alpha^2 \pi \rho_N \delta_{\alpha,\beta} \delta_{i,j}$. We have assumed that the densities of states of the normal metals are energy independent, i.e. $\rho_{e,a(b)} = \rho_{h,a(b)} \equiv \rho_N$. The symbol $\check{\vee}$ here denotes 4×4 matrices defined in the electrodes \oplus Nambu space, while we reserve the symbol \wedge for the reduced 2×2 Nambu space. To calculate \check{g} we first determine the superconductor surface Green function in momentum representation, $\hat{g}_S(E, k_y)$, using the asymptotic solutions of the Bogoliubov de Gennes equation [29], which yields

$$\hat{g}_S^r(E, k_y) = \frac{-2mi}{\hbar^2 D} \begin{pmatrix} \frac{1}{k^-} + \frac{\Gamma^2 e^{-i\Delta\varphi}}{k^+} & e^{i\varphi-} \left(\frac{\Gamma}{k_1} + \frac{\Gamma\delta}{k_2} \right) \\ e^{-i\varphi+} \left(\frac{\Gamma}{k_1} - \frac{\Gamma\delta}{k_2} \right) & \frac{1}{k^+} + \frac{\Gamma^2 e^{-i\Delta\varphi}}{k^-} \end{pmatrix} \quad (2)$$

where

$$\begin{aligned} k_\pm &= \sqrt{k_{xF}^2 \pm 2m\Omega/\hbar^2}, \quad \Gamma = |\Delta_+|/(E + \Omega) \\ \varphi_\pm &= \arg(\Delta_\pm), \quad \Delta\varphi = \varphi_+ - \varphi_-, \quad k_{xF}^2 = k_F^2 - k_y^2 \\ D &= (1 - \Gamma^2 e^{-i\Delta\varphi}), \quad \Omega = \sqrt{E^2 - |\Delta_+|^2} \\ \delta &= D(1 - e^{i\Delta\varphi})/(2 - 2\Gamma^2) \\ k_1^{-1} &= k_+^{-1} + k_-^{-1}, \quad k_2^{-1} = k_+^{-1} - k_-^{-1}. \end{aligned} \quad (3)$$

In the above equations Δ is the pair potential which depends on the wave vector, taking the values Δ_+ and Δ_- along the directions θ and $\pi - \theta$ respectively, where $\theta = \tan^{-1}(k_y/k_{xF})$. These are given by $\Delta_\pm(\theta) = \Delta_0$, for s symmetry and $\Delta_\pm = \Delta_0 \cos(2(\theta \mp \alpha))$ for d -symmetry. The retarded component is obtained by adding a small positive imaginary part $i\eta$ to the energy. From $\hat{g}_S(E, k_y)$ one then obtains the non-local components \hat{g}_{ba}^r by

$$\hat{g}_{ba}^r(E) = \int_{-\infty}^{\infty} \hat{g}_S^r(E, k_y) |f(k_y)|^2 e^{-ik_y d} dk_y, \quad (4)$$

where the weighting factor $f(k_y)$, proportional to the perpendicular wave vector k_{xF} , provides the appropriate connection between the continuous model used to describe the superconducting region and the discrete Hamiltonian approach used to obtain Eq. (1) (see Refs. [13, 30]).

As a first test of the model one can check that in the case of s -symmetry for $E < \Delta_0$ and $k_F d \gg 1$, $\sigma_{ba} \propto e^{-2d/\pi\xi} (\cos^2(k_F d) - \sin^2(k_F d))/d^3$ with $\xi(E) = \xi_0/\text{Re}(\sqrt{1 - E^2/\Delta^2})$ and $\xi_0 = \hbar v_F/(\pi\Delta_0)$, a result which agrees with Refs. [11, 13]. Therefore σ_{ba} exhibits changes in sign on the λ_F scale and its spatial average is zero [8, 12].

A. Results for $d_{x^2-y^2}$ symmetry

We now consider the $d_{x^2-y^2}$ symmetry. Due to the anisotropy of the pair potential an incoming electron from lead a is scattered as a quasiparticle in the superconductor, exploring regions where $E > \Delta(\theta)$ and $E < \Delta(\theta)$, with an effective coherence length $\xi(E, \theta) = \xi_0/\text{Re}(\sqrt{1 - E^2/\Delta(\theta)^2})$ which takes values from ξ_0 to ∞ . For this reason one typically finds that the propagators exhibit a slower decay with distance than in the case of s -symmetry. In this paper we have fixed $\Delta_0 \sim 20\text{meV}$ [31] and $\Delta_0/E_F \sim 10^{-1}$ as typical values for HTcS [32]. We also take $\eta \sim 0.002\Delta_0$ to simulate the effect of weak disorder [33]. Figure 2 illustrates the spatial dependence of the Green functions. Due to the dependence on k_y of

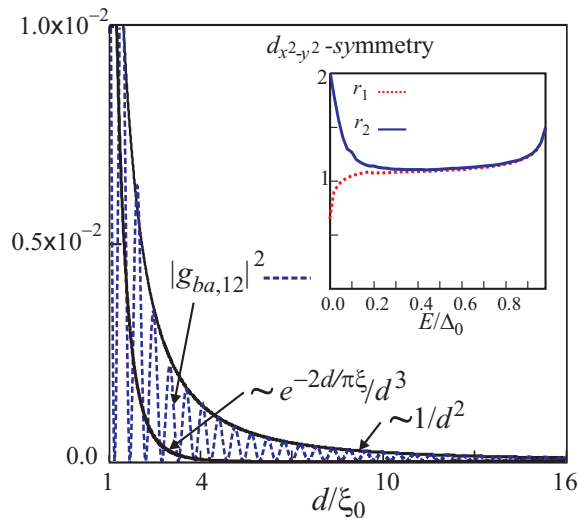


FIG. 2: (Color online) The anomalous propagator $|g_{ba,12}|^2$ for $d_{x^2-y^2}$ symmetry at zero energy as a function of the separation between the leads. The propagator has been normalized to its value in the normal state at $d = 0$. The corresponding electron propagator $g_{ba,11}$ is negligible within this scale. The envelope curve, decaying as $1/d^2$ is indicated by a full line. The corresponding curve for s -symmetry with the same choice of parameters, exhibiting an exponential decay, is also represented for comparison. The inset shows the exponents $r_{1,2}$ in the decay laws of Eq. (5) as a function of energy.

the pair potential, it is not possible to obtain an analytical expression of their variation with d as in the case of s symmetry. However, from numerical regressions for $k_F d \gg 1$, $|g_{ba,11}|^2$ and $|g_{ba,12}|^2$ can be fitted as

$$|g_{ba,11(12)}^r(E)|^2 \simeq \frac{c_{1(2)} + d_{1(2)} \cos^2(kd)}{|k_F d|^{r_{1(2)}}}. \quad (5)$$

The values of the exponents $r_{1(2)}$ fixing the spatial decay are shown in the inset of Fig.2 as a function of energy. For low energies ($E \ll \Delta_0$) $k \sim k_F$, $c_{1(2)} \ll d_{1(2)}$ and $d_2 \gg d_1 \rightarrow 0$ for $E \rightarrow 0$, and therefore the propagator $|g_{ba,12}^r|$ takes a much larger value than $|g_{ba,11}^r|$, yielding a clear dominance of CAR over EC in the tunnel limit. Notice that the low energy excitations at $\theta \sim \pi/4$ give a negligible contribution to $|g_{ba,11}^r|$ due to the weighting factor in Eq. (4) that is maximum at low angles. In contrast, most of the weight in $|g_{ba,12}^r|$ comes from $\theta \sim 0$ where Δ reaches a maximum. On the other hand, for energies higher than $E \sim 0.1\Delta_0$ $|g_{ba,12}^r|$ and $|g_{ba,11}^r|$ tend to have the same magnitude on average.

Fig. 3 further illustrates the different behavior of CAR and EC contributions to the non-local conductance for this orientation as one of the leads moves inside the superconductor while the second is located at the surface. These maps clearly correspond to a diffraction pattern for electrons injected at one point in the surface. In spite of its complex structure one can identify the region of low

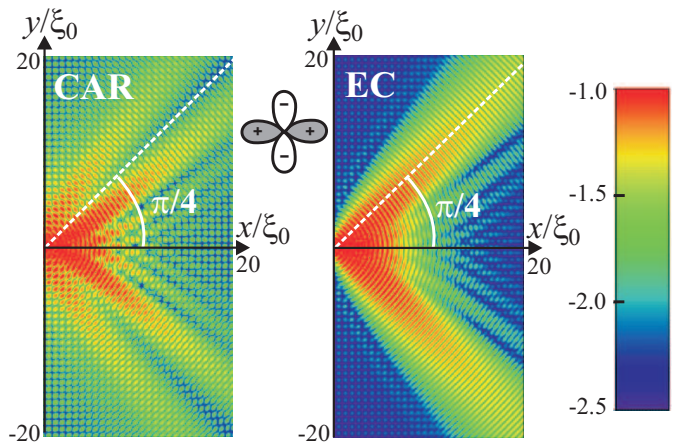


FIG. 3: (Color online) Plots of the CAR and EC contributions to the non-local conductance for the $d_{x^2-y^2}$ symmetry as one of the contacts moves inside the superconductor while the other remains fixed at $x = y = 0$. The contacts are in the tunnel limit and the voltage is set to zero. Both contributions are plotted in a logarithmic scale normalized to their maximum value.

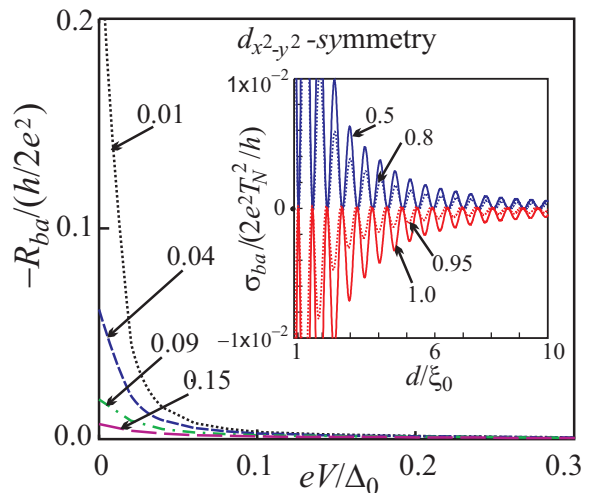


FIG. 4: (Color online) Spatial averaged non-local resistance at $d = 10\xi_0$ for $d_{x^2-y^2}$ symmetry as a function of the voltage for different values of the transmission T_N . The inset shows the non-local conductance at $eV = 0$ as function of d and for different values of T_N . For $T_N \approx 0.9$ there is a sign change in σ_{ba} .

angles from the surface ($\pi/2 > \theta \gtrsim \pi/4$) where CAR processes have a clear dominance and the nodal lines ($\theta \simeq \pi/4$) around which EC processes are favoured.

The results for σ_{ba} and R_{ba} in the $d_{x^2-y^2}$ orientation for arbitrary contact transmission are illustrated in Fig. 4. It is found that an increase in transmission leads to a reduction of the CAR contribution while the EC one increases. As a consequence both quantities exhibit a change of sign when the coupling to the leads increases.

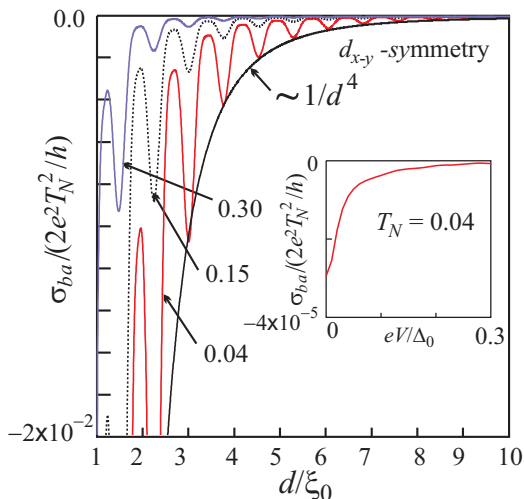


FIG. 5: (Color online) Non-local conductance at $eV = 0$ for d_{xy} symmetry as a function of the distance between the leads for $T_N = 0.04, 0.15$ and 0.3 . The inset shows the spatial averaged non-local conductance at $d = 10\xi_0$ and $T_N = 0.04$ as function of the voltage.

This is illustrated for σ_{ba} in inset of Fig. 4. We can obtain further insight on this effect at low energies where Eq. (1) can be approximated as

$$\sigma_{ba}(d) \simeq \frac{|1 - P^4 g_{aa,12}^{r2}|^2 - 4P^4 |g_{aa,12}^r|^2}{|1 + P^4 g_{aa,12}^{r2}|^4} |g_{ba,12}^r(d)|^2. \quad (6)$$

In obtaining this expression we have assumed symmetrical contacts ($p_a = p_b = p$) with $P = p\pi\rho_N$ being the normalized hopping parameter, such that the normal transmission for a single contact is $T_N = 4P^2/(1 + P^2)^2$. Within this approximation the dependence with the separation between the leads does not change when the transmission is increased, as it is seen in the inset of Fig. 4. On the other hand, this equation predicts a change in sign of σ_{ba} for $P \simeq 0.72$ ($T_N \simeq 0.9$) in agreement with the numerical results in the inset of Fig 4. The non-local resistance R_{ba} averaged on a range $\sim \lambda_F$ is shown in Fig. 4 for $d = 10\xi_0$. We observe that in the low transmission regime this quantity is negative, as it corresponds to the dominance of CAR processes, and exhibits a peak at low bias.

B. Results for d_{xy} symmetry

The results for d_{xy} -symmetry ($\alpha = \pi/4$) are shown in Fig. 5. The main effect for this symmetry is the appearance of a zero energy bound state [34], which is associated

with a $1/E$ dependence in $g_{ba,11}^r$. On the other hand, the distance dependence for low energy and $k_F d \gg 1$ is in this case approximately $1/d^4$ both for CAR and EC processes. In this orientation, the local Andreev reflection is zero because of diffraction of quasiparticles in the contact [35, 36] and the CAR contribution to σ_{ba} is not zero, but is always smaller than the EC one, leading to a negative non-local conductance as shown in Fig. 5. Basically, the dominance of the EC contribution is caused by the suppression of the pair potential along the $\theta = 0$ line. The effect of varying the contact transmission can be understood analytically within a similar approximation as done for the $d_{x^2-y^2}$ case, which allows to obtain the following expression for the crossed differential conductance

$$\sigma_{ba}(d) \simeq \frac{|g_{ba,12}^r(d)|^2 - |g_{ba,11}^r(d)|^2}{|1 + iP^2 g_{aa,11}^r|^4}. \quad (7)$$

Notice that CAR and EC contributions are equally affected by the coupling to the leads (through the P -dependent common denominator) and therefore EC dominates over CAR for the whole transmission range. The spatially averaged non-local conductance is negative and presents a zero bias peak that decreases with increasing transmission.

III. CONCLUSIONS

In summary we have analyzed the behavior of the crossed differential conductance in d -wave superconductors in a multiterminal configuration. We have shown that correlations between different leads exhibit an algebraical decay instead of the exponential behavior which is typically found in conventional superconductors. In the case of $d_{x^2-y^2}$ orientation crossed Andreev processes are favored at low voltages and contact transmissions, while for the d_{xy} case a zero bias non-local conductance peak appears, which is dominated by elastic-cotunneling. In both cases the spatially averaged non-local conductance is different from zero. These properties would allow to detect non-local transport at distances several times larger than the characteristic coherence length in these systems.

Acknowledgments

We thank H. Castro for fruitful discussions. Support by DIB of the Universidad Nacional de Colombia, the Spanish Ministerio de Ciencia e Innovacion through contract FIS2005-06255 and the EU program Nanoforum-EULA is acknowledged.

[1] P. Recher, E. V. Sukhorukov, and D. Loss, Phys. Rev. B **63**, 165314 (2001).

[2] N. M. Chtchelkatchev, G. Blatter, G. B. Lesovik, and

- T. Martin, Phys. Rev. B **66**, 161320 (2002).
- [3] C. Bena, S. Vishveshwara, L. Balents, and M. P. A. Fisher, Phys. Rev. Lett. **89**, 037901 (2002).
- [4] P. Recher and D. Loss, Phys. Rev. Lett. **91**, 267003 (2003).
- [5] P. Samuelsson, E. V. Sukhorukov, and M. Büttiker, Phys. Rev. Lett. **91**, 157002 (2003).
- [6] J. M. Byers and M. E. Flatté, Phys. Rev. Lett. **74**, 306 (1995).
- [7] G. Deutscher and D. Feinberg, Appl. Phys. Lett. **76**, 487 (2000).
- [8] D. F. G. Falci and F. W. J. Hekking, Europhys. Lett. **54**, 255 (2001).
- [9] D. Feinberg, Eur. Phys. J. B **36**, 419 (2003).
- [10] R. Mélin and S. Peysson, Phys. Rev. B **68**, 174515 (2003).
- [11] T. Yamashita, S. Takahashi, and S. Maekawa, Phys. Rev. B **68**, 174504 (2003).
- [12] R. Mélin and D. Feinberg, Phys. Rev. B **70**, 174509 (2004).
- [13] E. Prada and F. Sols, Eur. Phys. J. B **40**, 379 (2004).
- [14] A. Brinkman and A. A. Golubov, Phys. Rev. B **74**, 214512 (2006).
- [15] A. L. Yeyati, F. S. Bergeret, A. Martin-Rodero, and T. Klapwijk, Nat. Phys. **63**, 455 (2007).
- [16] M. S. Kalenkov and A. D. Zaikin, Phys. Rev. B **75**, 172503 (2007).
- [17] D. Beckmann, H. B. Weber, and H. v. Löhneysen, Phys. Rev. Lett. **93**, 197003 (2004).
- [18] S. Russo, M. Kroug, T. M. Klapwijk, and A. F. Morpurgo, Phys. Rev. Lett. **95**, 027002 (2005).
- [19] P. C. Zimansky and V. Chandrasekhar, Phys. Rev. Lett. **97**, 237003 (2006).
- [20] D. Beckmann and H. v. Löhneysen, Appl. Phys. A **89**, 603 (2007).
- [21] The dominance of CAR over EC processes is a necessary but not a sufficient condition to have an efficient entangler. For a more detailed discussion see Refs. [1, 2, 3, 4].
- [22] N. Stefanakis and R. Mélin, J. Phys.: Condens. Matter **15**, 4239 (2003).
- [23] S. Takahashi, T. Yamashita, and S. Maekawa, J. Phys. Chem. Solids **67**, 325 (2006).
- [24] I. Kosztin and A. J. Leggett, Phys. Rev. Lett. **79**, 135 (1997).
- [25] M. R. Li, P. J. Hirschfeld, and P. Wölfle, Phys. Rev. Lett. **81**, 5640 (1998).
- [26] P. Aronov and G. Koren, Phys. Rev. B **72**, 184515 (2005).
- [27] I. Asulin, O. Yuli, G. Koren, and O. Millo, Phys. Rev. B **74**, 092501 (2006).
- [28] J. C. Cuevas, A. Martin-Rodero, and A. L. Yeyati, Phys. Rev. B **54**, 7366 (1996).
- [29] W. J. Herrera, A. L. Yeyati, and A. Martin-Rodero, unpublished.
- [30] J. Bardeen, Phys. Rev. Lett. **6**, 57 (1961).
- [31] Ø. Fischer, M. Kugler, I. Maggio-Aprile, C. Berthod, and C. Renner, Rev. Mod. Phys. **79**, 353 (2007).
- [32] A. Golubov and F. Tafuri, Phys. Rev. B **62**, 15200 (2000).
- [33] This is consistent with the scattering rate at low temperatures extracted from surface impedance measurements in $YBaCuO$ see E. Farber et al. Physica C **317-318**, 550 (1999).
- [34] S. Kashiwaya and Y. Tanaka, Rep. Prog. Phys. **63**, 1641 (2000).
- [35] Y. Takagaki and K. H. Ploog, Phys. Rev. B **60**, 9750 (1999).
- [36] W. J. Herrera, J. V. Niño and J. J. Giraldo, Phys. Rev. B **71**, 094515 (2005).